Electron Paramagnetic Resonance Study of the Surface Hydration of Triton X-100 Micelles in Water with Added Monovalent Alkali Salts

Bissy Jude Jose, Barney L. Bales, and Miroslav Peric*

Department of Physics and Astronomy and The Center for Supramolecular Studies, California State University at Northridge, Northridge, California 91330-8268

Received: June 13, 2009; Revised Manuscript Received: August 19, 2009

The hydrophobic spin probe 2,2,6,6-tetramethyl-piperidin-1-oxyl-4-yl octadecanoate (TEMPO-stearate) was used to study the hydration of the polar shell of Triton X-100 micelles as functions of the concentration of the electrolytes KCl, NaCl, and LiCl and temperature. It was shown that the hydration of the polar shell of the Triton X-100 micelle decreases with both increasing electrolyte concentration and increasing temperature. The effect of Li^+ on the hydration of the polar shell was found to be smaller than those of Na^+ and K^+, which have almost identical behavior. The effective water concentration decreases from 18.3 to 15.8 M for LiCl and from 18.3 to 13.9 M for NaCl and KCl when the concentration of the electrolyte in the solution increases from 0 to 2.5 M. The dehydration of the polar shell was correlated to the average value of the cation hydration number calculated from literature data; the greater the cation hydration number, the greater the dehydration for the same increase in electrolyte concentration. Also, it was shown that the cloud point is strongly correlated to the hydration of the polar shell.

Introduction

((*p*-(1,1,3,3-Tetramethylbutyl)phenyl poly(ethylene glycol)), Triton X-100, is a nonionic surfactant that is extensively used to solubilize and purify transmembrane proteins.[1,2] Triton X-100 mixed micelle systems have also been successfully employed with numerous lipid-dependent enzymes in the study of surface dilution kinetics.[3−5] Due to its importance in biochemistry applications, the physicochemical properties of pure and mixed Triton X-100 micellar solutions have been studied with a wide range of techniques such as nuclear magnetic resonance (NMR),[6−8] quasi-elastic light scattering (QELS),[9,10,7] light scattering (LS),[11] time-resolved fluorescence quenching (TRFQ),[7] rotating disk electrode voltammetry,[12] small-angle X-ray scattering,[13] and viscometry.[14]

Recently, the growth and hydration of Triton X-100 micelles was studied as a function of the concentration of added electrolyte.[10−12] It was found that micelles become more compact with increasing electrolyte concentration, while at the same time there is an increase in the aggregation number of the micelle accompanied with an even greater increase in the amount of entrapped water at the periphery of the micelle.[12,11] It was suggested that the observed decrease in the partial specific volume with increasing electrolyte concentration is very likely caused by dehydration of the hydrophilic section of the micelle.[11] In other words, the hydrophilic polar shell of the micelle becomes dehydrated with the addition of electrolyte while the number of water molecules per surfactant increases.

The spin probe electron paramagnetic resonance (EPR) method has been used to study the surface hydration of sodium dodecyl sulfate (SDS) micelles as a function of electrolyte concentration.[15,16] The method relies on the sensitivity of the ^{14}N hyperfine coupling constant of a hydrophobic spin label probe to the average fraction of the volume occupied by water in the region of the nitroxide moiety that is located in the polar shell (hydrophilic part) of the micelle. The effective water concentration or hydration index[17] in the polar shell can be obtained through a calibration curve of the spin probe measured in a series of solutions of known hydration,[15,18] which then in turn may give the number of water molecules per monomer if the geometry of the micelle is well-known.[15,19,20] Also, the relative heights of the resonance lines give estimates of the rotational mobility of the spin probe yielding insights into the dynamic nature of the probe's environment.[21,18]

Since the substrate for studying the kinetics of lipid—dependent enzymes is usually solubilized by Triton X-100 micelles, and the enzyme activity strongly depends on the physicochemical properties of the polar shell,[3,4] such as surface hydration, it is important to gain a better understanding of the hydration state of the polar shell of Triton X-100 micelles.[22,23] The hydrophobic spin probe 2,2,6,6-tetramethyl-piperidin-1-oxyl-4-yl octadecanoate (TEMPO-stearate) has been used recently to study the interfacial properties of a variety of phosphatidylcholine vesicles[18] and of vesicles composed of the negatively charged dimyristoyl-phosphatidylglycerol (DMPG) and the zwitterionic dimyristoyl-phosphatidylcholine (DMPC) mixed with lysomyristoylphosphatidylcholine (LMPC).[19] TEMPO-stearate is very sparingly soluble in water, so it is certainly located in the Triton X-100 micelles. Although, a Triton X-100 micelle has a relatively large hydrophilic corona and a small (true) hydrophobic core, it is very likely that the hydrocarbon tail of the spin probe most of the time resides in the hydrophobic core, while the nitroxide moiety resides in the polar shell of the micelle. Therefore, TEMPO-stearate is an ideal spin probe for studying the interfacial properties of Triton X-100 micelles, because its location in the micelle is very likely the same as the location of the phospholipid molecule, so the nitroxide moiety senses a similar water concentration as the polar head of the phospholipid molecule.

The purpose of the present work is to study the hydration properties of the polar shell of Triton X-100 micelles using the spin probe EPR method, especially the effect of electrolyte, such

* Corresponding author. Tel.: 1 818 677-2944. Fax: 1 818 677-3234. E-mail: miroslav.peric@csun.edu.

10.1021/jp9055544 CCC: $40.75
Published on Web 09/16/2009

as KCl, NaCl, and LiCl, on the hydration of the polar shell of Triton X-100 micelles.

Experimental Section

Materials. The Triton X-100 surfactant was obtained from Sigma (Saint Louis, MI). The spin label TEMPO, 2,2,6,6-tetramethylpiperiden-1oxyl-4-yl octadecanoate (TEMPO-stearate), was obtained from Molecular Probes, Inc. (Eugene, OR). Monovalent alkali salts, NaCl, KCl, and LiCl, were purchased from Sigma Aldrich (Saint Louis, MI). The distilled water was purchased from Arrowhead (Arrowhead, CA). All chemicals were used as purchased.

The appropriate amount of TEMPO-stearate ethanol solution was added to a vial and then dried with a stream of N_2. Thereafter, a 25 mM water solution of Triton X-100 was added to the vial to produce a molar ratio [Triton X-100]/[spin probe] of 250; that is, all the samples had 0.1 mM of TEMPO-stearate in the presence of 25 mM Triton X-100. Each salt was added to this solution to achieve the desired concentration of electrolyte.

EPR Spectroscopy. EPR spectra were measured on a Bruker ESP 300 E spectrometer equipped with a Bruker variable temperature unit (Model B-VT-2000). Spin labeled Triton X-100 samples were prepared a day before the EPR measurements and stirred overnight. On the day of measurement, the samples, not degassed, were drawn into glass capillaries and sealed with a gas torch. The glass capillary was then placed into the Dewar within the EPR cavity. The temperature of the sample was controlled with a Bruker temperature unit and was stable within ±0.2 °C; the accuracy of the temperature was estimated to be within ±1 °C. Five EPR spectra were acquired, one after the other, employing a sweep time of 84 s; time constant, 20 ms; microwave power, 5 mW; sweep width, 50.2 G; and modulation amplitude, 1.0 G. The magnetic sweep width was measured with Bruker's NMR gaussmeter operating in the 1-mG resolution mode.

The EPR spectra were transferred from the spectrometer to a PC where they were analyzed by the computer program Lowfit. The Lowfit program is based on the fact that the ESR line shape, which is inhomogenously broadened due to unresolved hyperfine interaction, can be excellently described by a Lorentzian−Gaussian sum function.[24] One of the parameters that was obtained by the Lowfit analysis was the Lorentzian line width which was then used to calculate the rotational correlation times as described previously in ref 18. Since the TEMPO-stearate spin probe undergoes anisotropic Brownian rotational motion which is axially symmetric about an axis parallel to the hydrocarbon chain, one needs two independent rotational correlation times. Thus, one of the rotational correlation times $\tau_{||}$ characterizes the rotation of the spin probe about the stearate acyl chain symmetry axis, while the second rotational correlation time $\tau_{\perp}$ characterizes the rotation perpendicular to it. Since the rotational correlation times $\tau_{||}$ and $\tau_{\perp}$ characterize the rotation of the probe, which is sensitive to its surroundings, these quantities can give us useful information about the probe's environment.

The Lowfit program also gives precise values of the EPR line positions, which are used to calculate the nitrogen hyperfine coupling spacing A_+. A representative EPR spectrum of 0.1 mM TEMPO-stearate in 25 mM Triton X-100 micelles, its fit, and the definition of A_+ are given in the Supporting Information. The value of A_+ is sensitive to the amount of water in the probe's surroundings,[15,25,19] and therefore, it is a good measure of effective water concentration in the vicinity of the probe. The method for estimating the effective water concentration in the polar shell of Triton X-100 micelles is based on a calibration curve measured for TEMPO-stearate in a series of mixtures of ethanol−water and ethanol−1,4-dioxane covering the water fraction range in the solution from 0 to 0.8. The hydration index of each mixture,[17] defined as the ratio of the molar concentration of OH dipoles in the solution mixture to that of pure water can be easily evaluated.[25] Since the hydration index is a linear function of molar concentration of water, the effective water concentration is given by the following calibration equation:[18]

$$[H_2O] = \frac{A_+ - 15.542}{1.297} 55.345(M) \qquad (1)$$

where 55.345 M is the molar concentration of water with A_+ in Gauss.

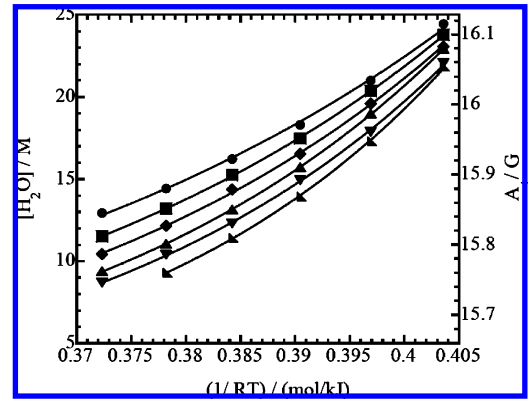

Figure 1. Effective water concentration $[H_2O]$ in the polar shell of 25 mM Triton X-100 micelles (left-hand ordinate) and corresponding nitrogen hyperfine spacing A_+ of 0.1 mM TEMPO-stearate (right-hand ordinate) as a function of $1/RT$. Symbols used to identify the different NaCl concentrations in Triton X-100 micelle solutions are the following: (circle) no NaCl; (square) 0.5 M NaCl; (diamond) 1.0 M NaCl; (up-pointing triangle) 1.5 M NaCl; (down-pointing triangle) 2.0 M NaCl; (lower-left-pointing triangle) 2.5 NaCl. Lines are the exponential fits $[H_2O] = [H_2O]_0 \exp(-\varepsilon_{H_2O}/RT)$ to the data, and the parameters $[H_2O]_0$ and $-\varepsilon_{H_2O}$ are given in Table 1. Error bars are standard deviations of five measurements and are about the same size as the symbols.

Results

The effective water concentration $[H_2O]$ sensed by TEMPO-stearate hyperfine and corresponding coupling spacing A_+ in the polar shell of the Triton X-100 micelles mixed with different concentrations of NaCl as a function of temperature are shown in Figure 1. As can be noted, the effective water concentration and the hyperfine coupling spacing decrease with increasing temperature, as well as with increasing electrolyte concentration. The experimental points can be fitted very well to the exponential expression $[H_2O] = [H_2O]_0 \exp(-\varepsilon_{H_2O}/RT)$, where $[H_2O]_0$ is the effective water concentration at $1/T = 0$, $-\varepsilon_{H_2O}$ is the activation energy for surface dehydration, and $R = 8.315$ J/mol·K is the gas constant; see the solid lines in Figure 1. The graphs of $[H_2O]$ and A_+ versus temperature with different electrolyte concentration, not shown here, for LiCl and KCl are very similar to Figure 1. Since the plots for all three electrolytes are the same in their general features, there is no need to display the other two plots. Thus, to save space, we use the exponential function to present our experimental data in Table 1. The values of the correlation coefficients R_c also attest to the goodness of the fits.

TABLE 1: Fitting Parameters $[H_2O]_0$ and $-\varepsilon_{H_2O}$ of Exponential Fits $[H_2O] = [H_2O]_0 \exp(-\varepsilon_{H_2O}/RT)$ and Correlation Coefficients R_c[a]

	NaCl			KCl			LiCl		
$C_{electrolyte}$, M	$[H_2O]_0 \times 10^5$ M	$-\varepsilon_{H_2O}$ kJ/mol	R_c	$[H_2O]_0 \times 10^5$ M	$-\varepsilon_{H_2O}$ kJ/mol	R_c	$[H_2O]_0 \times 10^5$ M	$-\varepsilon_{H_2O}$ kJ/mol	R_c
0.0	599	20.6	0.999	599	20.6	0.999	599	20.6	0.999
0.50	197	23.3	0.999	179	23.5	0.999	158	23.8	0.999
1.0	83.5	25.4	0.999	51.9	26.5	0.999	113	24.6	0.999
1.5	17.9	29.2	0.999	53.8	26.3	0.998	53.0	26.5	0.999
2.0	10.8	30.3	0.998	12.8	29.8	0.997	17.3	29.3	0.999
2.5	2.16	34.3	0.998	3.94	32.7	0.997	8.22	31.1	0.999

[a] $[H_2O]_0$ is the effective water concentration at $1/T = 0$, $-\varepsilon_{H_2O}$ is the activation energy for surface dehydration, and $R = 8.315$ J/mol·K is the gas constant.

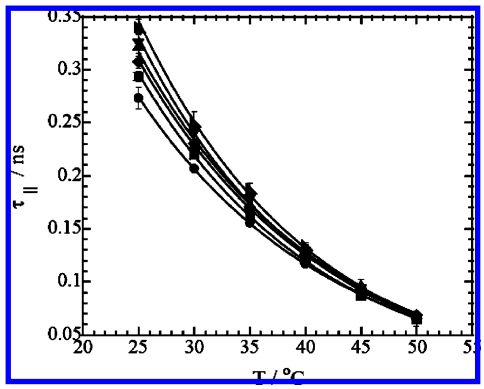

Figure 2. Parallel rotational correlation time $\tau_{||}$ of 0.1 mM TEMPO-stearate in the presence of 25 mM Triton X-100 as a function of temperature. Symbols used to identify the different NaCl concentrations in Triton X-100 micelle solutions are the following: (circle) no NaCl; (square) 0.5 M NaCl; (diamond) 1.0 M NaCl; (up-pointing triangle) 1.5 M NaCl; (down-pointing triangle) 2.0 M NaCl; (lower-left-pointing triangle) 2.5 NaCl. Lines are to guide the eyes and their parameters are given in Table 2. Error bars are standard deviations of five measurements.

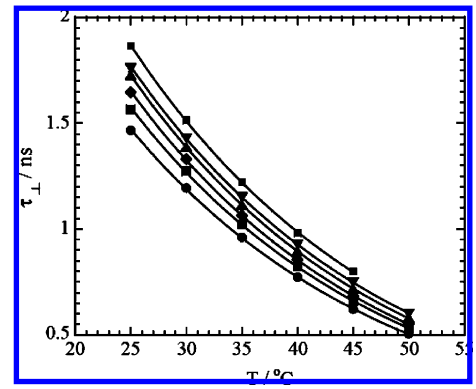

Figure 3. Perpendicular rotational correlation time $\tau_{\perp}$ of 0.1 mM TEMPO-stearate in the presence of 25 mM Triton X-100 as a function of temperature. Symbols used to identify the different NaCl concentrations in Triton X-100 micelle solutions are the following: (circle) no NaCl; (square) 0.5 M NaCl; (diamond) 1.0 M NaCl; (up-pointing triangle) 1.5 M NaCl; (down-pointing triangle) 2.0 M NaCl; (lower-left-pointing triangle) 2.5 NaCl. Lines are to guide the eyes and their parameters are given in Table 3. Error bars are standard deviations of five measurements and are about the same size as the symbols.

The rotational correlation times $\tau_{||}$ and $\tau_{\perp}$ characterize the axial rotation of the spin probe, which is affected by the physicochemical properties of the probe's surroundings. Therefore, those relaxation times can give us additional information about the water structure and dynamics in the polar shell of Triton X-100 micelles. Figure 2 shows the parallel rotational correlation time $\tau_{||}$, characterizing the rotation about the probe hydrocarbon chain, for Triton X-100 micelles as function of temperature for different concentrations of NaCl. As expected, the rotational correlation time $\tau_{||}$ decreases with increasing temperature, while the addition of NaCl increases the value of $\tau_{||}$.

Next, we present the perpendicular rotational correlation time $\tau_{\perp}$, characterizing the rotation of the nitroxide perpendicular to the hydrocarbon chain, as a function of temperature with different concentration of NaCl, Figure 3. Again, the rotational correlation time $\tau_{\perp}$ decreases with increasing temperature and becomes longer with the addition of electrolyte. The value of $\tau_{\perp}$ is greater than the value of $\tau_{||}$ for a given temperature at all temperatures, which is common for axial motion. Again, we do not show plots of experimental data for the rotational correlation times for KCl and LiCl. Instead, we present the experimental data using the fitting parameters A and b of exponential fits (Ae^{-bT}) to the data, where the parameters of the parallel rotational correlation time $\tau_{||}$ are given in Table 2, while the parameters of the perpendicular rotational correlation time $\tau_{\perp}$ are given in Table 3. As can be seen from Figures 2 and 3, and the correlation coefficients in Tables 2 and 3, the experimental data can be fitted extremely well to an exponential function. As far as we know, the fitting function used for the $\tau_{||}$ and $\tau_{\perp}$ data does not have any physical meaning; it is just a good fit to the experimental data.

Discussion

Experimental methods such as NMR,[8] QELS,[9,10] LS,[11] rotating disk electrode voltammetry,[12] small-angle X-ray scattering,[13] and viscometry[14] measure the total number of water molecules associated with Triton X-100 micelles. By contrast, the spin probe EPR method measures the effective water concentration sensed by the nitroxide moiety in its surroundings.[18,19,25,21] Therefore, in order to clearly understand the results of this work, it is necessary to compare the effective water concentration, in other words, the effective number of water molecules measured by the spin probe EPR method to those hydration values measured by other methods. Since the spin probe EPR method measures water in the immediate proximity of the probe, while some hydrodynamic methods measure water in a more extended region, we have to be very careful when comparing the same quantities measured by those methods. That is, data gathered by different methods very often sense different regions and might be painting somewhat different pictures.

The effective water concentration $[H_2O]$ can be easily found from the measured hyperfine splitting A_+, eq 1, which can be

TABLE 2: Fitting Parameters A and b of Exponential Fits (Ae^{-bT}) to the Parallel Rotational Correlation Time Data for Different Concentrations of Electrolyte and Correlation Coefficients R_c

	NaCl			KCl			LiCl		
$C_{electolyte}$ M	A ns	b 1/°C	R_c	A ns	b 1/°C	R_c	A ns	b 1/°C	R_c
0	1.14	0.0570	0.999	1.14	0.0570	0.999	1.14	0.0570	0.999
0.5	1.349	0.0606	0.999	1.398	0.0603	0.999	1.366	0.0596	0.999
1.0	1.393	0.0602	0.999	1.490	0.0613	0.999	1.495	0.0619	0.999
1.5	1.434	0.0604	0.999	1.556	0.0624	0.999	1.528	0.0607	0.999
2.0	1.642	0.0641	0.999	1.774	0.0658	0.999	1.694	0.0623	0.999
2.5	1.732	0.0644	0.999	1.551	0.0605	0.998	1.794	0.0628	0.999

then converted into the number of water molecules per surfactant sensed by the spin probe n_W^{SP} according to the following equation:

$$\frac{[H_2O]}{55.345\ M} = \frac{n_W^{SP} V_W}{n_W^{SP} V_W + V_{OE}} \quad (2)$$

where $V_W = 30$ Å^3 is the volume of a water molecule and $V_{OE} = 637$ Å^3 is the volume of the ethylene oxide group.[26] Although the location of the spin probe is well-known, that is the hydrocarbon tail is in the hydrocarbon core of the Triton X-100 micelle and the nitroxide moiety is in the polar shell of the micelle, the range of motion of the nitroxide is not, which introduces an uncertainty when the effective water concentration is converted into number of water molecules. This uncertainty was discussed in more detail in ref 19. Here, we assume that the nitroxide moiety samples the volume that is equal to the volume of the ethylene oxide (EO) group plus the volume of the water molecules surrounding the OE group, the denominator in eq 2. We also assume that the addition of salt does not noticeably change the relative position of the spin probe and Triton X-100 molecules. The effective numbers of water molecules calculated from the effective water concentration presented in Figure 4 (full squares) for pure Triton X-100 micelles at different temperatures are given in Table 4. Hydration numbers for pure Triton X-100 micelles have been reported to be in the range of 20−50 water molecules.[12] Taking into account that other methods measure both the water in the polar shell and the water hydrodynamically associated with the micelles, while our method measures only the water molecules in the polar shell, it is not surprising that our hydration numbers are slightly smaller and, as such, are in very good agreement with previously reported numbers. Note that we avoid identifying the water sensed by nitroxide to what other authors call hydrogen bound water.[12,11] Since the nitroxide moiety is very likely located in the polar shell, the water sensed by nitroxide is slightly less than the hydrogen bound water and as long as the micelle does not undergo drastic structural changes, it is a good measure of that water.

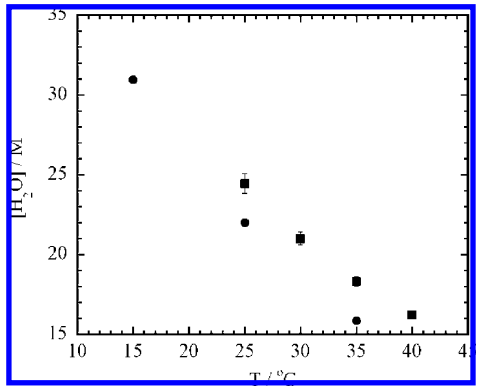

Figure 4. Effective water concentration $[H_2O]$ in the polar shell as a function of temperature. Full circles are the values calculated from the geometry of the Triton X-100 micelle using eq 3, and full squares are the measured values (Table 4). Error bars are standard deviations of five measurements.

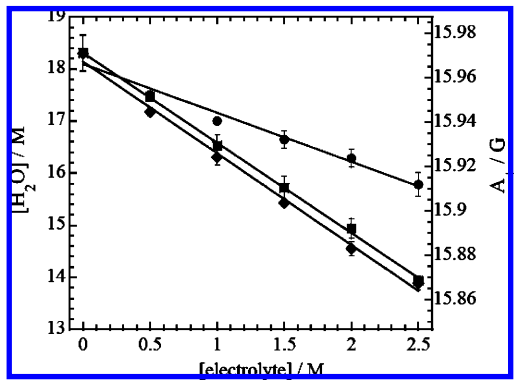

Figure 5. Effective water concentration $[H_2O]$ in the polar shell of 25 mM Triton X-100 micelles calculated from eq 1 (right-hand ordinate) and corresponding nitrogen hyperfine coupling constant A_+ of 0.1 mM TEMPO-stearate (left-hand ordinate) as a function of electrolyte concentration at 35 °C. Symbols used to identify the different electrolyte in Triton X-100 micelle solutions are the following: (circle) LiCl, (square) NaCl, (diamond) KCl. Error bars are standard deviations of five measurements.

The water concentration in the polar shell of globular structures such as micelles can be calculated from the geometrical parameters of the micelle and the surfactant and the aggregation number[15,21,19] by

$$[H_2O] = \frac{V_S - V_H}{V_S} 55.345[M] \quad (3)$$

where V_S is the volume of the polar shell of the micelle and $V_H = N_{agg} V_{OE}$ is the volume of all the surfactant heads in the polar shell. V_S is given by $4\pi r_0^3/3 - N_{agg} V_{hg}$, where r_0 is the effective radius of the micelle and V_{hg} is the volume of the hydrophobic group of a Triton X-100 molecule. In other to further validate our method, we use the radius of the Triton X-100 micelle from Table 2 in ref 14, and the aggregation number (143 molecules) and the volumes of the hydrophobic (363 Å^3) and hydrophilic (637 Å^3) parts of Triton X-100 reported by Robson and Dennis[26] to calculate the effective water concentration in the polar shell of the Triton X-100 micelle. The calculated $[H_2O]$ (full circles) together with measured $[H_2O]$ (full squares) are presented in Figure 4. As can be seen, the agreement is very good, and the temperature dependence of $[H_2O]$ is the same, which means that the spin probe EPR method can successfully be used to study the effective water concentration in Triton X-100 micelles as a function of both electrolyte concentration and temperature.

TABLE 3: Fitting Parameters *A* and *b* of Exponential Fits (Ae^{-bT}) to the Perpendicular Rotational Correlation Time Data for Different Concentrations of Electrolyte and Correlation Coefficients R_c

	NaCl			KCl			LiCl		
$C_{electolyte}$	*A* ns	*b* 1/°C	R_c	*A* ns	*b* 1/°C	R_c	*A* ns	*b* 1/°C	R_c
0	4.304	0.0429	0.999	4.304	0.0429	0.999	4.304	0.0429	0.999
0.5	4.653	0.0434	0.999	4.619	0.0428	0.999	4.804	0.0432	0.999
1.0	4.955	0.0440	0.999	4.829	0.0429	0.999	4.881	0.0434	0.999
1.5	5.123	0.0438	1.0	4.869	0.042	0.999	5.101	0.0427	0.999
2.0	5.185	0.0430	0.999	4.947	0.041	0.999	5.424	0.0432	0.999
2.5	5.410	0.0426	0.999	5.186	0.0423	0.999	5.655	0.0432	0.999

TABLE 4: Effective Water Concentration and Number of Water Molecules Sensed by the Spin Probe in the Polar Shell of the Triton X-100 Micelle at Different Temperatures

T/°C	$[H_2O]$/M	n_W^{SP}/no. water mol/EO group
25	24.4	16
30	20.9	12.5
35	18.0	10
40	16.2	8.5

The effective water concentration in the polar shell of the Triton X-100 micelle decreases with increasing temperature, Figures 1 and 4, as well as with increasing electrolyte concentration, Figure 1. In other words, the polar shell gets dehydrated with an increase in both temperature and electrolyte concentration. The good exponential fits indicate that the dehydration process is an activated process, and the fact that $-\varepsilon_{H_2O}$ is positive means that the process is spontaneous; in other words, the water molecules transferring from the polar shell to the aqueous micellar surroundings do not encounter a potential barrier, but do fall into a potential well. Also, it can be clearly seen that the activation energy is directly proportional to the concentration of electrolyte, Table 1. Several authors have observed a decrease in intrinsic viscosity with increasing electrolyte concentration, which indicates a decrease in specific micellar volume. The decrease in specific micellar volume was then attributed to collapse of the EO chains due to dehydration.[12,11] Micellar surface dehydration was also inferred from a decrease of area per surfactant with increasing electrolyte concentration.[11] Obviously, our observation of micellar surface dehydration is in good agreement with those previously reported.

We present a plot of the hyperfine splitting and effective water concentration of Triton X-100 micelles as a function of electrolyte concentration at 35 °C for NaCl, KCl, and LiCl, Figure 5. The plots at other temperatures are similar. From Figure 5, it is obvious that dehydration is more pronounced in the presence of NaCl and KCl than LiCl. The effective water concentration decreases from 18.3 to 15.8 M when the concentration of LiCl in the solution increases to 2.5 M, while for the same mole increase of NaCl and KCl the value of $[H_2O]$ decreases to 13.9 M. In terms of water molecules, calculated by eq 2, the presence of 2.5 M LiCl in the solution reduces the number of water molecules per EO group from 10 to 8, whereas the presence of the same concentration of the other two electrolytes reduces the number of water molecules from 10 to 6.8.

To see how the presence of an electrolyte affects the motion of nitroxide, that is the parallel and perpendicular rotational times, we present $\tau_{||}$, Figure 6, and $\tau_{\perp}$, Figure 7, as a function of electrolyte concentration at 35 °C for all three electrolytes. As expected, the values of both $\tau_{\perp}$ and $\tau_{||}$ increase with increasing electrolyte concentration indicating the dehydration of the hydrophilic shell of the micelle. Again, the effect of LiCl is quite different than that of the other two electrolytes, but this time the effect of LiCl is greater than the effect of NaCl and KCl. The fact that the values of $\tau_{\perp}$ and $\tau_{||}$ are longer in the presence of LiCl indicates that the structure of water molecules in the polar shell of the micelle is slightly more rigid which might be explained by possible forming of complexes between Li^+ and Triton X-100 molecules.[27] Na^+ and K^+ do not form complexes with polyoxyethylated surfactants.[27]

One of the macroscopic properties of a nonionic surfactant is its cloud point, which is the temperature where the surfactant solution starts to separate into two phases making the solution look cloudy.[12,11] Molina-Bolivar et al.[11] and Charlton and Doherty[12] showed that the cloud point was reduced with increasing electrolyte concentration due to salting out behavior. The presence of cations in the aqueous solution decreases the water concentration in the polar shell, so the number of hydrogen bonds formed with the ether groups decrease, which in turn reduces the barrier for micelle−micelle interactions. The final result of salting-out is that the micelle−micelle interaction becomes more likely and the cloud

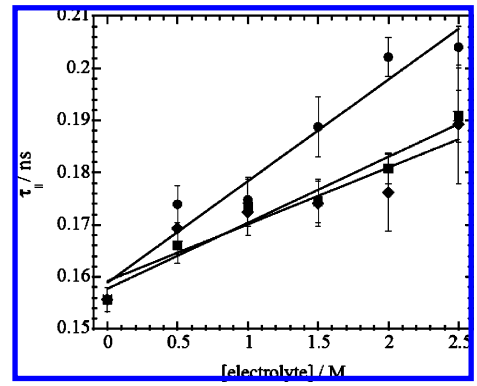

Figure 6. Parallel rotational correlation time $\tau_{||}$ of 0.1 mM TEMPO-stearate in the presence of 25 mM Triton X-100 as a function of electrolyte concentration at 35 °C. Symbols used to identify the different electrolytes in Triton X-100 micelle solutions: (circle) LiCl, (square) NaCl, (diamond) KCl. Error bars are standard deviations of five measurements.

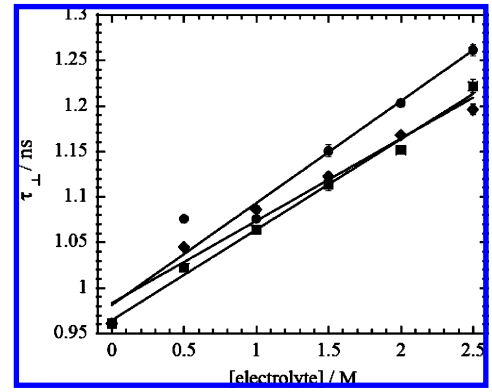

Figure 7. Perpendicular rotational correlation time $\tau_{\perp}$ of 0.1 mM TEMPO-stearate in the presence of 25 mM Triton X-100 as a function of electrolyte concentration at 35 °C. Symbols used to identify the different electrolyte in Triton X-100 micelle solutions: (circle) LiCl, (square) NaCl, (diamond) KCl. Error bars are standard deviations of five measurements and are about the same size as the symbols.

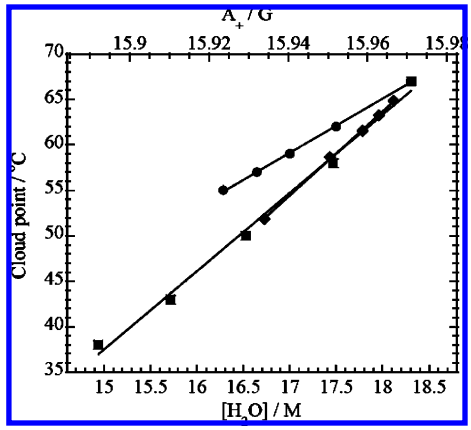

Figure 8. Cloud point of Triton X-100 as a function of effective water concentration [H_2O] in the polar shell of 25 mM Triton X-100 micelles at 35 °C (lower abscissa) and corresponding nitrogen hyperfine spacing A_+ of 0.1 mM TEMPO-stearate (upper abscissa). Symbols used to identify the different electrolyte in Triton X-100 micelle solutions: (circle) LiCl, (square) NaCl, (diamond) KCl.

point decreases. Since the EPR method measures the effective water concentration in the polar shell, we present a plot of cloud point versus effective water concentration (lower axis) and hyperfine coupling constant (upper axis) for all three electrolytes in Figure 8. The data for the cloud points of Triton X-100 in the presence of NaCl and LiCl are taken from Figure 4 of ref 11 and in the presence of KCl from Figure 5 of ref 12. As can be seen, there is an almost perfect linear relation between cloud point and [H_2O] for all three electrolytes. Notice that the addition of LiCl lowers the cloud point much less than the addition of the other two electrolytes. Charlton and Doherty[12] suggested that the effect of Na^+ and K^+ on cloud points should be identical. Thus, it is not at all surprising that the data for NaCl and KCl in Figure 8 overlap.

Although a large number of published reports have been devoted to the most accurate determination of the hydration numbers of ions by a variety of methods,[28] the reported numbers for any given ion have a wide range of values, and are dependent on the methods of measurement. For these reasons, Israelachvili stated in his book:[29] "The hydration number is more of a qualitative indicator of the degree to which ions bind water rather than an exact value." Table 1 in ref 28 contains the hydration numbers of Li^+ measured by diffraction methods in the range 4−6, or in terms of average value and standard deviation, 4.3 ± 0.7; the hydration numbers of Na^+ measured by diffraction methods are in the range 4−8 or 5.6 ± 1.7; the hydration numbers of K^+ measured by diffraction methods are in the range 4−8 and one measurement of 2.2 and 3.2, or after averaging 5.0 ± 1.6. Statistically, the average value of a quantity is a better representation of the quantity than any individual measurement. Therefore, it is very likely that the dehydration of the micellar surface is related to the hydration (coordination) number of the cations, because the average value of the hydration number of Li^+ is obviously lower than the other two, which are statistically very close. This implies that even in the case of Li^+ the hydration of the polar shell of the micelle in part depends on the cation hydration, and not just on the formation of complexes between Li^+ and Triton X-100. In summary, the statement by Molina-Bolivar et al.[11] that the hydration of the polar shell of the micelle decreases with increasing electrolyte concentration can now include Li^+.

Conclusions

The experimental EPR data presented here have clearly shown that the hydration of the polar shell of the Triton X-100 micelle depends strongly on the concentration and the nature of the electrolyte added to the micellar solution. An increase in the concentration of electrolyte increases the dehydration of the hydrophilic part of the Triton X-100 molecules. The dehydration of the polar shell is much smaller in the case of Li^+ than in the case of Na^+ and K^+, while the dehydration due to Na^+ and K^+ is identical. The presence of 2.5 M LiCl in the Triton X-100 solution reduces the number of water molecules per EO group from 10 to 8, whereas the presence of the same concentration of the other two electrolytes reduces their number from 10 to 6.8. This result is reasonably well-correlated to the average value of the hydration of cations calculated from literature data. Also, it was shown that the polar shell hydration is strongly correlated to the cloud point for all three electrolytes, as expected.

Acknowledgment. The authors gratefully acknowledge support from NIH Grant S06 GM48680 (B.L.B. and M.P.).

Supporting Information Available: Fitting of an EPR spectrum. This material is available free of charge via the Internet at http://pubs.acs.org.

References and Notes

(1) Alberts, B.; Bray, D.; Lewis, J.; Raff, M.; Roberts, K.; Watson, J. D. *Molecular Biology of the Cell*, third ed.; Garland Publishing, Inc.: New York, 1994.
(2) Lasch, J. *Biochim. Biophys. Acta* **1995**, *1241*, 269.
(3) Carman, G. M.; Deems, R. A.; Dennis, E. A. *J. Biol. Chem.* **1995**, *270*, 18711.
(4) Deems, R. A. *Anal. Biochem.* **2000**, *287*, 1.
(5) Deems, R. A.; Eaton, B. R.; Dennis, E. A. *J. Biol. Chem.* **1975**, *250*, 9013.
(6) Ribeiro, A. A.; Dennis, E. A. *Biochemistry* **1975**, *14*, 3746.
(7) Brown, W.; Rymdik, R.; van Stam, J.; Almgren, M.; Svensk, G. *J. Phys. Chem.* **1989**, *93*, 2512.
(8) Sadaghiani, A. S.; Khan, A. *Langmuir* **1991**, *7*, 898.
(9) Streletzky, K.; Phillies, G. D. J. *Langmuir* **1996**, *11*, 42.
(10) Phillies, G. D. J.; Yambert, J. E. *Langmuir* **1996**, *12*, 3431.
(11) Molina-Bolivar, J. A.; Aguiar, J.; Carnero Ruiz, C. *J. Phys. Chem. B* **2002**, *106*, 870.
(12) Charlton, I. D.; Doherty, A. P. *J. Phys. Chem. B* **2000**, *104*, 8327.
(13) Paradies, H. H. *J. Phys. Chem.* **1980**, *84*, 599.
(14) Mandal, A. B.; Ray, S.; Biswas, A. M.; Moulik, S. P. *J. Phys. Chem.* **1980**, *84*, 856.
(15) Bales, B. L.; Messina, L.; Vidal, A.; Peric, M.; Nascimento, O. R. *J. Phys. Chem.* **1998**, *B 102*, 10347.
(16) Bales, B. L.; Shahin, A.; Lindblad, C.; Almgren, M. *J. Phys. Chem. B* **2000**, *104*, 256.
(17) Mukerjee, P.; Ramachandran, C.; Pyter, R. A. *J. Phys. Chem.* **1982**, *86*, 3189.
(18) Alves, M.; Peric, M. *Biophys. Chem.* **2006**, *122*, 66.
(19) Alves, M.; Bales, B. L.; Peric, M. *Biochim. Biophys. Acta* **2008**, *1778*, 414.
(20) Ranganathan, R.; Peric, M.; Medina, R.; Garcia, U.; Bales, B. L.; Almgren, M. *Langmuir* **2001**, *17*, 6765.
(21) Peric, M.; Alves, M.; Bales, B. L. *Chem. Phys. Lipids* **2006**, *142*, 1.
(22) Kumbhakar, M.; Nath, S.; Mukherjee, T.; Pal, H. *J. Chem. Phys.* **2004**, *121*, 6062.
(23) Kumbhakar, M.; Goel, T.; Mukherjee, T.; Pal, H. *J. Phys. Chem. B* **2004**, *108*, 19246.
(24) Bales, B. L. Inhomogeneously Broadened Spin-Label Spectra. In *Spin Labeling: Theory and Applications*; Berliner, J. L., Reuben, J., Eds.; Plenum: New York, 1989; Vol. 8, p 77.
(25) Peric, M.; Alves, M.; Bales, B. L. *Biochim. Biophys. Acta* **2005**, *1669*, 116.
(26) Robson, R. J.; Dennis, E. A. *J. Phys. Chem.* **1977**, *81*, 1075.
(27) Schott, H.; Royce, A. E.; Han, S. K. *J. Colloid Interface Sci.* **1984**, *98*, 196.
(28) Ohtaki, H.; Radnai, T. *Chem. Rev.* **1993**, *93*, 157.
(29) Israelachvili, J. N. *Intramolecular and Surface Forces - With Applications to Colloidal and Biological Systems*; Academic Press: London, 1985.

JP9055544